Post-eruptive sedimentary processes in volcanic crater lakes: implications for deciphering the Samoan sedimentary record

A. Fepuleai, S. J. Gale, N. A. Wales, S. P. L. McInerney, K. K. Lal & B. V. Alloway

Journal of Paleolimnology

ISSN 0921-2728

J Paleolimnol
DOI 10.1007/s10933-018-0035-y

Springer

J Paleolimnol
https://doi.org/10.1007/s10933-018-0035-y

ORIGINAL PAPER

Post-eruptive sedimentary processes in volcanic crater lakes: implications for deciphering the Samoan sedimentary record

A. Fepuleai · S. J. Gale · N. A. Wales · S. P. L. McInerney · K. K. Lal · B. V. Alloway

Received: 27 July 2017 / Accepted: 25 May 2018

Abstract The two largest islands of the Samoan chain, Savai'i and Upolu, possess almost 400 volcanic cones. Their craters form enclosed, internally drained basins that potentially retain long, detailed and uninterrupted sedimentary sequences. Because of the sparsity, fragmentary nature and low temporal resolution of records of environmental change from the tropical Pacific, these deposits have the potential to fill an important gap in our knowledge of global climatic and environmental change. To interpret such records we must understand the depositional processes that operate in these basins. Unfortunately, although the post-eruptive sedimentology of volcanic calderas and maars is relatively well-established, that of crater lakes remains poorly understood. The volcanic edifice of Mount Lanotō in southeast Upolu was selected for investigation. The form of the volcano and its crater are typical of those observed across the island. The sediments retained in the crater are composed largely of plant-organic-rich muds that display little visible evidence of stratigraphic variation. Mineral magnetic and chemical methods were therefore employed to document the types and distribution of sedimentary facies represented in the post-eruptive crater fill and, by inference, the processes of sedimentation that had operated in the crater. The earliest post-eruptive deposits are the result of the failure of the crater's oversteepened internal slopes. The crater floor subsequently collapsed to form a pit crater. The basal deposits in the pit crater are likely to be the product of the collapse of its walls and roof. However, the bulk of the material in the feature was laid down under lacustrine conditions. These deposits accumulated in a relatively deep-water environment. Across the rest of the accumulation zone, by contrast, water levels appear to have been shallow. Sedimentation during this phase was dominated by autochthonous plant-organic-rich deposits, with minor fine-grained clastic input. Deposition was intermittently interrupted by localised episodes of mass movement that reworked the regolith mantling the steep internal slopes of the crater into the accumulation zone in the form of low-angle fans. At the broad scale, the sedimentology of

A. Fepuleai · N. A. Wales · K. K. Lal
School of Geography, Earth Science and Environment, The University of the South Pacific, Suva, Fiji

S. J. Gale (✉)
Department of Archaeology, The University of Sydney, Sydney, NSW 2006, Australia
e-mail: sgal8292@uni.sydney.edu.au

S. P. L. McInerney
School of Education, University of Technology Sydney, Sydney, NSW 2007, Australia

B. V. Alloway
School of Environment, The University of Auckland, Private Bag 92019, Auckland 1142, New Zealand

B. V. Alloway
Centre for Archaeological Science, School of Earth and Environmental Sciences, University of Wollongong, Wollongong, NSW 2522, Australia

Published online: 05 June 2018

Lake Lanotō displays similarities with that of volcanic calderas and maar lakes. However, the morphological simplicity of the basin, the general absence of contemporaneous volcanic activity, the timing of the onset of lacustrine conditions, the derivation of the clastic deposits in the volcanic crater almost solely from the by-products of the volcanic eruption, and the high biological activity in the lake waters mean that there are important differences between the types and distribution of sedimentary facies identified in Lake Lanotō and those represented in models of deposition in maars and volcanic calderas.

Keywords Pacific · Samoa · Quaternary · Volcanic crater lake · Sedimentation · Magnetic susceptibility

Introduction

Efforts to reconstruct global climatic and environmental change are hindered by the existence of great tracts of the Earth where paleoenvironmental records are sparse to non-existent. Perhaps the largest and most significant of these is that of the Pacific (O'Reilly et al. 2015; PAGES2k Consortium 2017). This is a region that lies at the frontier of paleoenvironmental research, in part a consequence of its limited land area and the consequent restriction in the number of sites available to trap and preserve depositional records of environmental change. Given this context, the large number of enclosed volcanic basins throughout the Samoan island chain is of considerable significance, for these features have the potential to retain long, detailed and uninterrupted archives of environmental change in an area where records are sparse, fragmentary and of low temporal resolution.

The Samoan volcanic lineament is located in the South Pacific between latitudes 11°S and 15°S and longitudes 168°W and 178°W (Fig. 1). The subaerial part of the lineament extends from Savai'i in the west to Ta'u in the east. East of Ta'u, the chain continues through the seamounts of Vailulu'u and Malulu to the atoll of Rose Island, whilst to the southeast of Tutuila, a long submarine ridge culminates in the young volcano of Malumalu. West of Savai'i, the Samoan chain may be represented by a string of seamounts and submarine banks. Although these do not form a single lineament, Hart et al. (2004) have identified a Samoan geochemical signature in those seamounts up to 750 km west of Combe Reef.

The landscapes of the two largest islands of the Samoan island chain, Savai'i and Upolu, are predominantly the product of late Quaternary basaltic volcanism (Kear and Wood 1959). On both islands, the younger volcanic terrain is notable for the presence of large numbers of volcanic cones, in excess of 50 on Upolu and around 320 on Savai'i. These generally form enclosed, internally drained basins that act as sediment traps and offer considerable potential for the retention of valuable sedimentary records of environmental change. Despite this, the only attempt to exploit this capability has been that of Parkes (1994), who studied an incomplete core of Holocene sediments from Lake Lanoto'o in the centre of Upolu.

A critical first step in interpreting these records is to understand the depositional processes that operate in these basins. Almost all the Samoan lakes lie in former vents within volcanic cones, making them true crater lakes in the sense of Timms (1992) and Christenson et al. (2015), rather than related features such as maars, diatremes or calderas. Although the infill of crater lakes has been widely investigated as a source of paleoenvironmental information (Holmgren et al. 2012; Öberg et al. 2012), the sedimentary processes that occur within them are not well understood. By contrast, the sedimentology of lakes in maars and volcanic calderas has been closely examined. Nelson et al. (1994), for example, proposed a conceptual model of deposition in caldera basins. Despite being based on work in a limited set of environments (largely Crater Lake, Oregon, USA and a handful of similar lakes elsewhere in the Americas), this model has been widely invoked as an archetype of caldera sedimentation (Larsen and Crossey 1996; Cohen 2003; Otake 2007; Jiang et al. 2012; Murphy et al. 2016). The model was developed in the context of small ($\leq$ 10 km diameter) calderas, although it is thought to be applicable in a range of other situations, including impact and explosion craters. The model has four stages:

1. Stage 1 is that of caldera subsidence. This results in the formation of a ring fracture zone along the margins of the collapsed volcanic edifice. The fracture zone provides a focus for subsequent volcanic activity in the caldera and forms deep

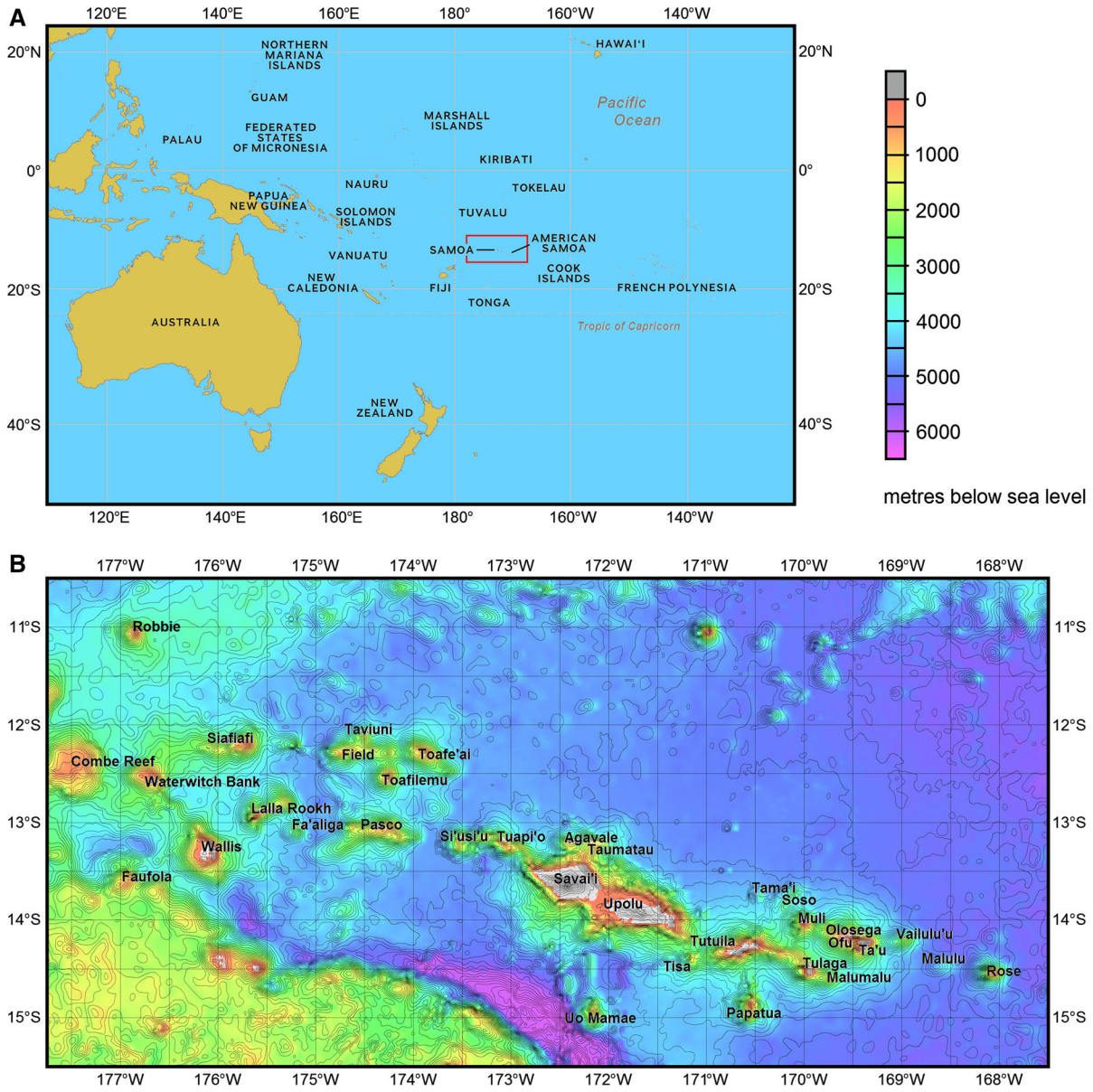

Fig. 1 **a** The western Pacific Ocean, showing the location of the Samoan volcanic lineament. **b** The bathymetry of the Samoan volcanic lineament. Bathymetric and topographic contours at 200 m intervals. The base map is from EarthRef (2006)

basins that control the pattern of sedimentation on the caldera floor.

2. Stage 2 begins with a brief phase of sheetwash deposition, although subsequent sedimentation is dominated by mass-transport processes that deposit debris wedges that thin towards the basin centre. These range from kilometre-scale avalanches from the caldera wall to local debris fans that may be only a few hundred metres long. Localised volcanic activity along the ring fracture zone takes place concurrently with the failure of the caldera walls. The environment within which these processes operate is subaerial and Stages 1 and 2 both occur prior to substantial lake sedimentation.
3. In Stage 3, the basin experiences rapid flooding and the development of fully lacustrine conditions. The subaerial debris wedges are replaced by

flat-lying, well-bedded turbidites, which fill the sub-basins in the caldera floor. Diatomaceous lacustrine muds drape volcanic features that continue to form concurrently with lake sedimentation. Seismic activity associated with volcanic eruption may trigger slope failure, resulting in the formation of thick and coarse turbidite beds that cover the entire floor of the basin. Lava domes may intrude the sediments and disrupt lake deposition.

4. In Stage 4, major volcanic activity ceases. Lake sedimentation is focussed in small basins with multiple local sediment sources. Base-of-slope turbidite aprons grade to basins infilled by flat-lying muds, whilst local subaerial and subaqueous debris flows deposit coarse-grained material at the base of the caldera walls and around the margins of the basins.

More recent studies have complicated, but not significantly altered, the picture presented by this model. Heiken et al. (2000), investigating the Creede Caldera in Colorado, USA, stressed the contribution of ash falls, pyroclastic flows and travertine deposits to lake sedimentation, and the role of resurgent volcanic dome formation in confining deposition to a moat located between the caldera wall and the dome. Murphy et al. (2016) investigated Long Valley Caldera in California, USA. They emphasised the role of resurgent dome formation in providing a source of sediments to the lacustrine sequence and noted the development of Gilbert-type deltas during the final stage of caldera sedimentation.

By contrast with calderas, maars tend to have simpler eruptive histories. Their formation is usually the result of a single, short-lived explosive event. The effects of subsequent volcanism are limited to the deposition of tephra from regional sources and the interruption of deposition by late-magmatic-phase lava (Cohen 2003; Lorenz 2007). Maars are small and generally have simple sub-circular forms (Ollier 1967; Ross et al. 2011). Their craters are cut into the country rock and are surrounded by a rim of pyroclastic debris (Lorenz 1973). Maar craters commonly intersect the water table and evidence from those maars that have formed in historic times suggests that craters fill rapidly with water after, or even during, eruption (White and Ross 2011). Their smaller catchments and simpler forms tend to yield less complex patterns of sedimentation. Despite this, many of the features of post-caldera sedimentation are replicated in maar basins. Thus, the earliest post-eruptive deposits often consist of tens of metres of relatively coarse material formed by the collapse of the crater walls and the deposition of debris fans and debris flows. These are succeeded by fine-grained lacustrine deposits (White 1989; White and Ross 2011). The fill may experience subsidence (White and Ross 2011) and deposition may be interrupted by volcanic activity (Lorenz 2007). Maar lakes are usually isolated from the surrounding environment by the pyroclastic rim. Occasionally, however, part of the rim collapses, providing a pathway for sediments to enter the crater; Gilbert-type fans may develop where streams are able to gain access to the basin (White 1992).

Cohen (2003) has suggested that maar sedimentation typically consists of relatively simple accumulations of four facies types:

1. Narrow (typically < 100 m wide) marginal aprons of coarse gravel composed of the rock that makes up the crater walls.
2. Turbidites derived from the margins of the crater.
3. Fine-grained, often laminated, lake sediments, containing siliciclastic, carbonate, diatomaceous and/or plant-organic debris.
4. Episodic beds of volcanic ash derived from regional sources (Guo et al. 2005).

Pirrung et al. (2003) have proposed a model of maar crater sedimentation based on observations in the Tertiary Central European Volcanic Fields. The basal lithozone consists of a breccia composed of uncemented fragments of largely unweathered country rock. This is thought to be the product of in situ fragmentation or the collapse of the crater walls, probably before any cover of maar tephra exists on the landscape. Lithozone B consists of carbonate-cemented fragments of weathered country rock and weathered lapilli. This represents either slides of base surge and wallrock collapse material or the product of post-eruptive collapse of the crater walls.

Lithozone C consists of a complex alternation of beds of unsorted silt- to gravel-grade material and well-sorted silts and sands, along with lithologically diverse breccias of pyroclasts, and weathered and unweathered country rock. These are thought to represent post-eruptive debris flows and turbidites.

Lithozone D is dominated by fine clastic deposits. These grade upwards from laminated minerogenic silts containing frequent debris flow deposits to laminated plant-organic-rich silts containing gravelly debris flows and turbidites. These represent deposition under fully lacustrine conditions.

Lithozone E consists of gyttja and peat deposits. These represent the final stage of lake development in its evolution through swamp conditions to dry land.

The aim of this project was to investigate the deposits found in volcanic crater lakes in Samoa in order to understand the post-eruptive depositional processes that operate in these basins and thus decipher their sedimentary record. In addition, we sought to add to the limited amount of information on sedimentation in volcanic crater lakes and to place this in the context of the far-better-understood models of sedimentation in maars and volcanic calderas.

Study site

The island of Upolu is approximately 72 km long and 25 km wide, with a broadly lenticular form aligned east-southeast (Fig. 2). A linear upland chain, rising to an altitude of 1100 m, runs along the main axis of the island, whilst to the north and northeast lie detached areas of deeply dissected upland terrain. The island is composed almost entirely of Late Pliocene–Holocene basalts (Kear and Wood 1959).

The oldest rocks, the Fagaloa Volcanics of Late Pliocene–Early Pleistocene age (Natland and Turner 1985; Workman et al. 2004; McDougall 2010), form an eroded basement that is exposed on the northeastern and southwestern sides of the island and at a handful of locations where rivers have trenched gorges through the stratigraphically higher rocks. Unconformably overlying the Fagaloa rocks are olivine basalts of late Quaternary age (Kear and Wood 1959). These form primary volcanic landforms that include lava fields, valley fills and monogenetic spatter and scoria cones. To the north and northeast, the lavas abut and surround the dissected uplands of the Fagaloa rocks. Elsewhere, the landscape is dominated by a series of volcanic craters and cones developed along the east-southeast axis aligned along the crest of the island (Fig. 2). Dana (ca 1849) and Stearns (1944) regarded the chain of craters and cones as marking a rift zone from which the younger volcanic rocks had been erupted. The lavas appear to have flowed north and south from the island axis, infilling pre-existing valleys and forming lobate features, some of which extend out over the surrounding reefs.

The site selected for study was the volcanic edifice of Mount Lanotō in the southeast of Upolu (Fig. 2). The form of the volcano and its crater are typical of those observed across the island. Its basin is entirely enclosed, effectively trapping sediment generated within its catchment and minimising the potential for

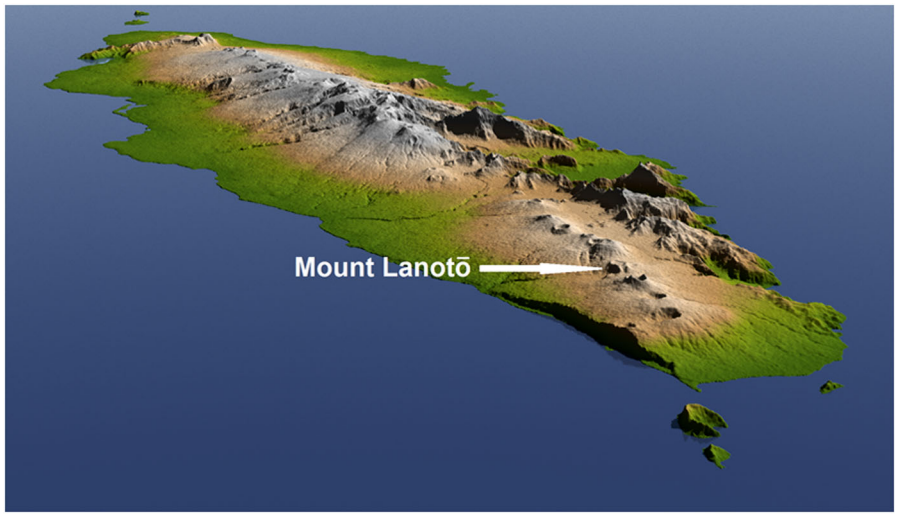

Fig. 2 The island of Upolu, Samoa from the southeast, showing the location of Mount Lanotō. Image size approximately 75 km by 75 km (Image PIA1196: elevation data acquired by the Shuttle Radar Topography Mission, a National Aeronautics and Space Administration, National Geospatial-Intelligence Agency and Jet Propulsion Laboratory co-operative project)

the disruption and interruption of its sedimentary record. Its crater lake is relatively deep and apparently permanent, capable of trapping and preserving sediment and limiting the loss or modification of the depositional record by erosion and weathering. The catchment is small and its internal slopes are short and steep. Transport routes between the catchment slopes and the depositional basin are therefore few and efficient. This reduces the potential for sediment storage on the slopes and encourages a rapid and near-complete transmission of material mobilised on the catchment to the sediment sink. This is likely to minimise any lag in sedimentary response to events in the catchment and the broader environment. The sedimentary record may therefore represent a near-complete and near-instantaneous response to events in the catchment area. Lake Lanotō thus has the capacity to preserve a long, detailed and uninterrupted record of environmental history that is reflective of conditions throughout the Samoan island chain. More broadly, its sediments may contribute to our understanding of environmental shift in the tropical Pacific and help fill an important gap in our knowledge of global climatic and environmental change.

Mount Lanotō is a compound volcano (Fig. 3), consisting of two overlapping volcanic centres and their associated eruptive products, located along the central axial rift of the island. The main body of the feature is a 2-km-diameter, sub-circular cone, reaching more than 150 m above the surface of the surrounding lava fields and elongate along a southeast by east axis. The flanks of the cone rise up to a sharp divide from which slopes descend steeply to a flat-bottomed, interior basin (Fig. 4). Extending along the axis to the southeast is a secondary rift-like crater. This is narrower than the main cone and does not possess a flat base, but has similarly steep sides and internal slopes. Like the main crater, the rift forms a closed basin, with no topographic outlet either to the main basin or the surrounding lava fields.

The form of the volcanic cone of Mount Lanotō appears little modified by erosion: the crater rim is unbroken and of even height, and there is little evidence of fluvial dissection of either the inner or outer slopes. Notwithstanding this, the inner slopes are somewhat scalloped (Fig. 5), possibly indicative of slope failure and the mass movement of material into the crater.

At the centre of the flat-bottomed interior basin of the main crater is a lake. This has a sub-circular form and very steep sides, plunging to depths of over 4 m within a short distance of its rim (Fig. 6). It appears to have a relatively flat bottom and to contain at least 6 m of sediment. By contrast, the topography of the surrounding swamp is subdued, with elevated, vegetated hummocks separated by water-filled hollows, with an overall relief of around 1 m. The interior slopes of the crater rise sharply from the floor of the basin to the rim of the cone. The slopes are thickly forested and appear to possess a continuous soil cover. No exposures of bedrock were observed, although occasional boulders of basalt are found towards the base of the slopes.

The forest vegetation on the interior slopes of the crater consists of perhaps 16 species, dominated by the tree fern, *Cyathea lunulata* (with an estimated relative dominance of 21%), the palm, *Clinostigma* cf. *warburgii* (19%), a native nutmeg, *Myristica hypargyraea* (15%), *Cyathea affinis* (15%) and *Trichospermum richii* (12%). Almost all these trees and tree ferns are characteristic of secondary forest in Samoa.

The swamplands of the flat-bottomed interior basin of the main crater are dominated by *Eleocharis dulcis* (water chestnut), with notable quantities of *Lycopodium cernuum* (club moss), *Dicranopteris linearis* (false staghorn fern), *Cyclosorus interruptus* (a marsh fern) and a species of moss that forms a layer beneath the taller herbaceous species. The combination of *Eleocharis* and *Cyclosorus* is typical of lowland marshes in Samoa. The elevated hummocks, by contrast, are dominated by the stunted tree species, *Metrosideros collina*, *Spiraeanthemum samoense* and *Fagraea berteroana* (all typical of primary montane forest), *Pandanus turritus* (an endemic species of screwpine that is also characteristic of primary montane forest), *Scirpodendron ghaeri* (a large marsh sedge) and the shrub *Melastoma denticulatum*. Several fern species, such as *Nephrolepsis hirsutula*, are also present. This is not typically found in wetlands, but is able to survive on the slightly elevated topography of the hummocks. The description of the vegetation in the Lake Lanotō basin is based on observations made on 30 July 1996 (W. A. Whistler, pers. commun. 2018).

The pit in which Lake Lanotō is found is likely to have a volcanic origin, with processes such as eruption, explosion and subsidence all potentially

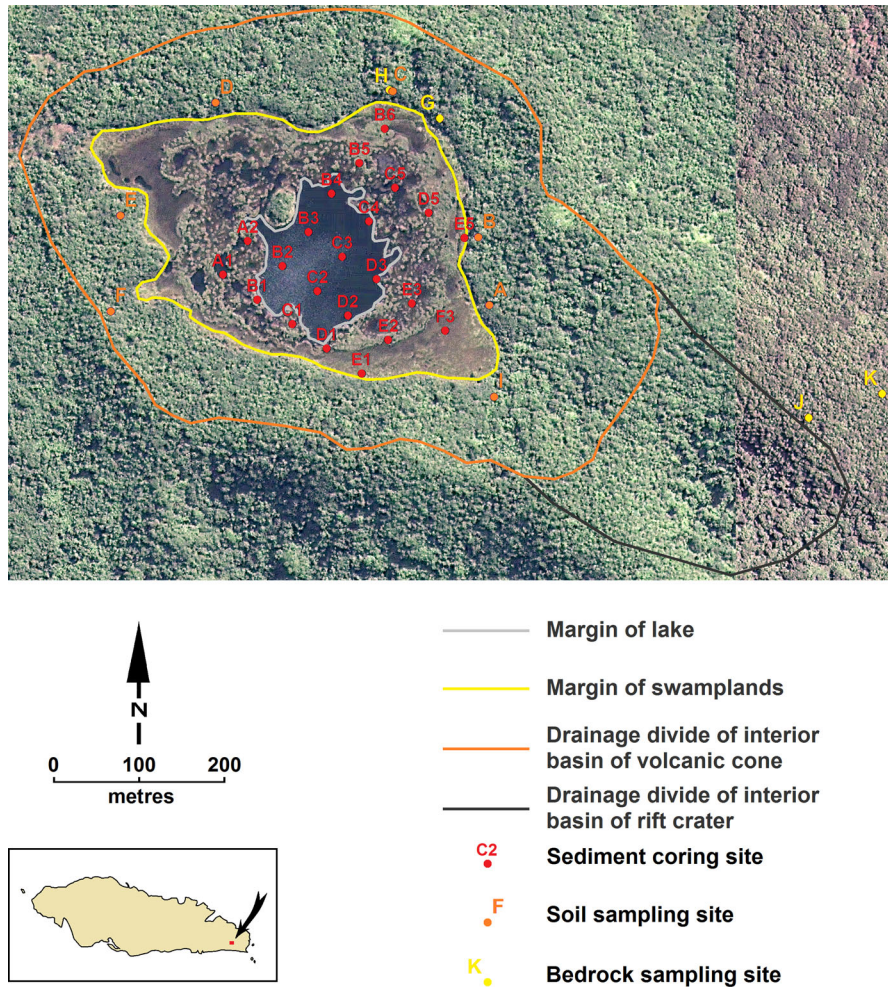

Fig. 3 Mount Lanotō, southeast Upolu, Samoa, showing the catchments of the volcanic cone and the rift crater, the interior slopes of the volcanic cone, and the basal swamplands and lake. The image also shows the locations of the sediment coring sites and the soil and bedrock sampling sites. The 2011 DigitalGlobe© imagery was supplied by the Secretariat of the Pacific Community (SPC) Geoscience Division

involved. However, there is no trace across the interior basin of the elevated rim, the radial distribution of pyroclastic debris or the lava flows that are associated with eruption vents or explosion pits (Wyrick et al. 2004; Németh and Cronin 2008). It is possible that some of these features may lie buried beneath the later basin-fill deposits. It is also possible that the products of explosive activity may have been reworked back onto the basin flats from the inner slopes of the crater. Nevertheless, there is no evidence, either in the cores taken across the basin or on the slopes surrounding the swamplands, of eruption or explosion deposits that postdate the formation of the crater.

Instead, it is possible that the feature is a pit crater formed within the main interior basin by the collapse of the surface above a void, such as a lava tube or a drained magma chamber. Pit craters are thought to propagate upwards by a process of stoping. Newly formed craters have steep overhanging sides and become wider with depth. With time, however, the overhangs collapse and the craters take on a cylindrical form. Continuing collapse results in the outward expansion of the crater and the development of a funnel-like shape. Pit craters are typically located along rift zones, have an elliptical planform, steep, overhanging or talus-covered bedrock walls, and a

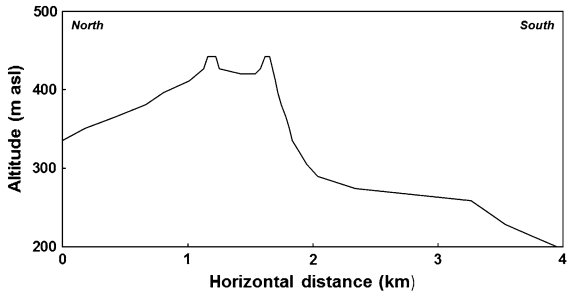

Fig. 4 North–south cross-section through Mount Lanotō, southeast Upolu, Samoa along meridian 171°29′38″W, showing the development of the volcanic cone on a gently sloping lava surface (data from Department of Lands and Survey, Western Samoa 1978)

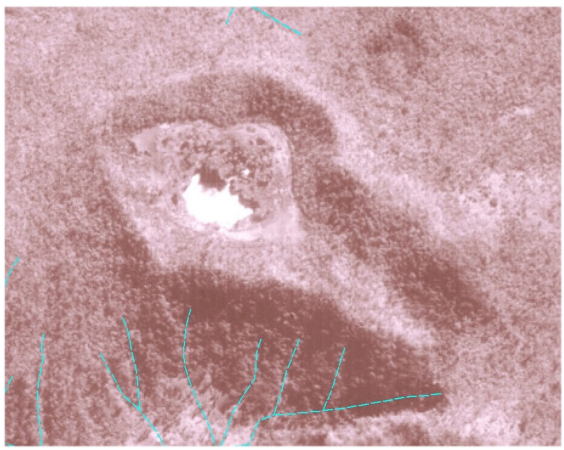

Fig. 5 Mount Lanotō, southeast Upolu, Samoa. The imagery was supplied by the National Mapping Section, Ministry of Natural Resources and Environment, Apia, Samoa

characteristic width:depth ratio; whilst the elevated rim associated with eruption vents and explosion pits is typically absent (Okubo and Martel 1998). Although its infill precludes determination of the true depth of the feature, Lake Lanotō possesses several characteristics of pit craters. It has steep walls, almost certainly composed of bedrock, an elliptical morphology and a location along the major east-southeast-aligned rift zone that runs the length of the island.

Although meteorological measurements from Apia on the north coast of Upolu began in 1890, the location of the observatory was shifted in 1902 and some records are incomplete (Solofa and Aung 2004). The values reported here are therefore World Meteorological Organisation averages for the period 1971–2000. Temperatures varied little during this time. Mean

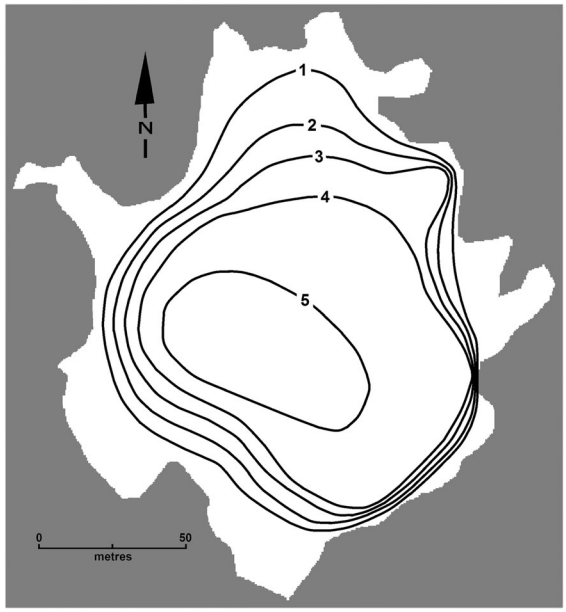

Fig. 6 The bathymetry of Lake Lanotō, southeast Upolu, Samoa. Bathymetric contours in metres

monthly minima ranged from 22.6 °C in July to 24.2 °C in February, whilst mean monthly maxima varied from 29.5 °C in July to 30.7 °C in April. The mean annual rainfall was 2965 mm, with a drier winter (the mean precipitation in August was 113 mm) and a wet summer (the mean precipitation in January was 489 mm). The climate of Upolu lies within the Af (wet tropical with no dry season) category of Köppen's (1936) climatic classification.

Annual average potential evapotranspiration for the period 1960–1986 at Apia was 1584 mm and average rainfall during that time exceeded average potential evapotranspiration during every month of the year (Burgess ca 1987). The water balance is probably even more favourable in the southeast of the island, where Lake Lanotō is located, and where the mean annual rainfall is likely to be > 3500 mm (Burgess ca 1987).

Materials and methods

For the purposes of sampling, the main crater basin was divided into two sectors: the basal wetlands, in which sediments were thought to accumulate, and the steep interior slopes of the crater, across which erosional processes were considered to dominate (Fig. 3). The wetlands cover an area of 0.10 km^2,

the interior slopes extend over 0.29 km^2. The slopes were sampled by taking bulk samples of the upper 0.15 m of the soil profile from seven sites (Fig. 3). Since no bedrock outcrops were observed within the crater, it was not possible to obtain in situ samples of substrate material. Instead, several boulders, which can only have been derived from the inner slopes of the crater, were sampled (Fig. 3). Samples were taken for analysis from the interior, unweathered components of these boulders. In addition, samples were collected from recent excavations that exposed the bedrock walls of the secondary rift-like crater of the volcano (Fig. 3).

The deposits of the accumulation zone were sampled on a 50 m grid aligned along the main axis of the crater (Fig. 3). Percussion cores up to 6.65 m in length were extracted from 22 sites using either 55 mm or 90 mm external diameter polyvinyl chloride tubing (note that the core from site A2 was only partially recovered). The depth of water and the thickness of sediment penetrated were recorded at each coring site. Preliminary inspection of the accumulation zone sediments revealed them to be composed largely of plant-organic-rich muds that display little visible evidence of stratigraphic variation. Measurements of volume-specific magnetic susceptibility were therefore employed to identify spatial and vertical changes in sediment character. Volume-specific magnetic susceptibility is the ratio of the magnetisation induced in a material to the strength of the applied magnetic field. The use of plastic tubing allowed downcore variations in volume-specific magnetic susceptibility to be measured without extruding the cores from their sleeves. Measurements were taken at 20 mm intervals along each core, following procedures similar to those described by Gale and Hoare (2011).

Using this information, it was possible to trace stratigraphic features across the entire lake basin. Since sediment stratigraphies could be readily correlated, only a single site needed to be studied in detail. The longest- and highest-resolution record came from site D3, located on the southeast side of Lake Lanotō (Fig. 3). This was therefore chosen as the site of the master core, on which most of the analyses were undertaken.

The barrel of core D3 was opened by making longitudinal cuts on opposite sides of the sleeving. One section of sleeve was removed to expose the deposits without disturbing them. The core was sampled in a series of 20-mm-thick spits (n = 219). Care was taken to avoid sampling sediment in contact with the barrel wall to minimise the risk of contamination by material dragged down the walls of the pipe during the coring process. The core slices and the soil samples were dried at 90 °C for 24 h. The dried samples were split to provide subsamples for mineral magnetic, chemical and loss on ignition analysis. Cylinders 25 mm in height and 20 mm in diameter were cut from each bedrock sample for measurement of their magnetic properties. The < 2 mm fraction of one of the splits from each of the soil and sediment samples was packed into weighed 2.5 cm^3 polyethylene vials. Low-field mass-specific magnetic susceptibility and frequency-dependent magnetic susceptibility were measured on the bedrock specimens and on each soil and sediment split following the procedures outlined by Gale and Hoare (2011). Mass-specific magnetic susceptibility is determined by expressing volume-specific magnetic susceptibility in terms of sample mass. Frequency-dependent magnetic susceptibility is the change in susceptibility as a function of the frequency of the applied field. Specifically, it is the increase in susceptibility per factor of ten reduction in the frequency of the applied magnetic field, as a proportion of the initial susceptibility. The measure provides information on the grain size of the magnetic carriers.

Bulk samples of the rocks and the < 2 mm fraction of the second of the splits from each of the soil and sediment samples were ground to a fine powder using a tungsten carbide ring-and-puck mill. Approximately 1.0000 g of each powder was digested in a combination of hot concentrated HNO_3 and HCl following the procedures outlined by Gale et al. (2006). The elemental chemistry of the digestates was determined by inductively coupled plasma spectrometry. A further $\approx$ 1.0000 g of each powder was ignited at 430 °C for 24 h using the methods described by Gale and Hoare (2011) to estimate the plant-organic content of the materials.

Results

Sediments of the accumulation zone

The main volcanic crater of Mount Lanotō consists of two distinct landforms: steep, forest-clad slopes that descend from the narrow crater rim, and a flat-bottomed base, composed of swamplands surrounding a steep-sided lake. The slopes appear to be dominated by erosional processes and to be places where material is subject to weathering, entrainment and, ultimately, removal. The basal wetlands appear to be governed by sediment accumulation. In the absence of evidence for quantitatively significant accumulations of tephra or other products of atmospheric fallout in the basin, it is likely that the atmospheric contribution to sedimentation in the accumulation zone is small and that its sediments are derived almost entirely from within the catchment. Since this is the case, three possible sources of depositional input to the accumulation zone can be identified. The first is the lake and the surrounding swamplands, in which accumulate autochthonous materials that include the chemical and organic deposits of wetland environments. Secondly, there are the soils and other regolith materials developed on the slopes surrounding the accumulation zone. Finally, although it is poorly exposed and largely seen in the form of boulders reworked down the catchment slopes, there is the bedrock of which the crater walls are composed.

There are probably no sites within the basin where deposition is entirely the product of autochthonous processes. Those locations in the deepest parts of the lake that are most distant from sources of allochthonous input are the most likely to be dominated by local material. Our analyses of core D3 were therefore employed to obtain a record of autochthonous deposition in the basin. Despite the likely contribution of allochthonous material to this site, these deposits will be employed here, with suitable caveats, for that purpose.

The lake sediments generally display low magnetic susceptibility (Figs. 7, 8). This is likely to reflect the accumulation of plant-organic material in the sediments (loss on ignition values range from 19.4 to 69.3% by mass) and the dilution of the susceptibility signal by high concentrations of diamagnetic plant matter.

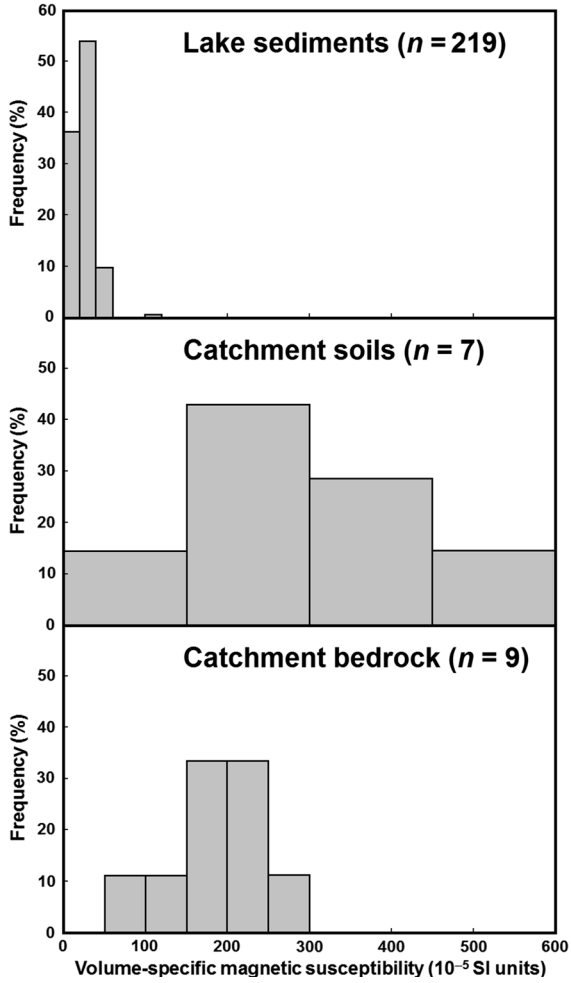

Fig. 7 The frequency distribution of the volume-specific magnetic susceptibility of the lake sediments, soils and bedrock from Mount Lanotō, southeast Upolu, Samoa. The lake sediments are from core D3. The location of the soil and bedrock sampling sites is shown in Fig. 3

The bedrock has moderately-high susceptibility, typical of basic volcanic rocks (Gale and Hoare 2011) and suggestive of high concentrations of ferrimagnetic minerals (Figs. 7, 8). Typically, the frequency-dependent susceptibility (X_{fd}) of basalts is low (Pollard et al. 1998; Dearing 1999). By contrast, the values observed here are moderately high, although comparable and higher values have been reported for apparently unweathered Quaternary basalts by Mena et al. (2006). Moderate values of bedrock X_{fd} are usually interpreted as indicative of superparamagnetism resulting from the presence of secondary magnetic minerals produced as a by-product of weathering

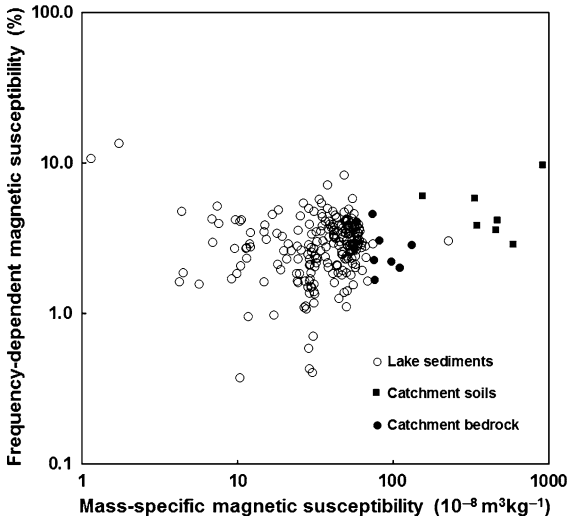

Fig. 8 The mass-specific and frequency-dependent magnetic susceptibility of the lake sediments, soils and bedrock from Mount Lanotō, southeast Upolu, Samoa. The lake sediments are from core D3. The location of the soil and bedrock sampling sites is shown in Fig. 3

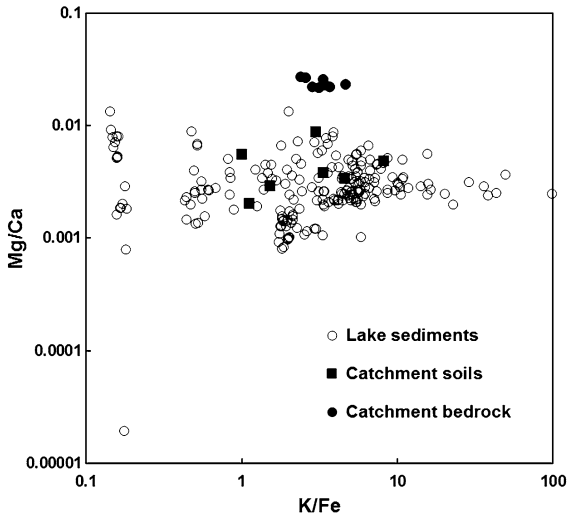

Fig. 9 The ratios of K/Fe and Mg/Ca in the lake sediments, soils and bedrock from Mount Lanotō, southeast Upolu, Samoa. The lake sediments are from core D3. The location of the soil and bedrock sampling sites is shown in Fig. 3

(Gale and Hoare 2011), although de Wall and Worm (2000–2001) have suggested that that the frequency dependence of basalts may be associated with the presence of titanomagnetites (or coarse-grained pyrrhotites or hematites).

The soils display high magnetic susceptibility, indicative of substantial concentrations of ferrimagnetic minerals (Figs. 7, 8). The relatively high values of frequency-dependent magnetic susceptibility are indicative of the presence of fine-grained secondary ferrimagnetic minerals. Taken together, these measures are suggestive of the operation of some process of susceptibility enhancement, such as burning or pedogenesis (Gale and Hoare 2011).

The major element chemistry of the three groups of potential source materials is summarised in Fig. 9. Whilst the catchment bedrock can be distinguished from the other potential sediment sources, there is a notable overlap between the chemical properties of the soils and the lake sediments.

The stratigraphy of the accumulation zone

Downcore variations in volume-specific magnetic susceptibility in the cores taken across the interior basin of the main crater allow the reconstruction of the stratigraphy of the basin fill (Fig. 10). The patterns are complex, displaying considerable variation in both magnitude and configuration. The sequences obtained from the lake itself (B2–B4, C2–C4 and D2–D3) can be distinguished from those of the surrounding swamplands. The lacustrine cores possess a consistent stratigraphy that can be traced laterally across the lake and vertically to depths > 6 m. Figure 11 shows the broad pattern of stratigraphic ties between these cores, whilst Fig. 12 shows the detailed correlations for the deepest cores on each of the three transects across the lake. The stratigraphic integrity displayed by the lacustrine cores strongly suggests that the deposits are undisturbed and that they are likely to preserve a coherent record of environmental change.

The stratigraphy of the swamp deposits, by contrast, is highly variable, displaying complex patterns and substantial shifts in susceptibility from core to core. Nevertheless, the maximum values of volume susceptibility recorded in each core reveal a consistent trend, with the highest values found around the margins of the depositional basin and the lowest values within the lake itself (Fig. 13).

The thickness of the high-susceptibility unit (defined as constituting all parts of the core exhibiting values of volume-specific magnetic susceptibility $\geq 190 \times 10^{-5}$ SI units) within each swamp core also appears to decrease with distance into the accumulation zone. This is seen in the relationship between the thickness of the high-susceptibility unit

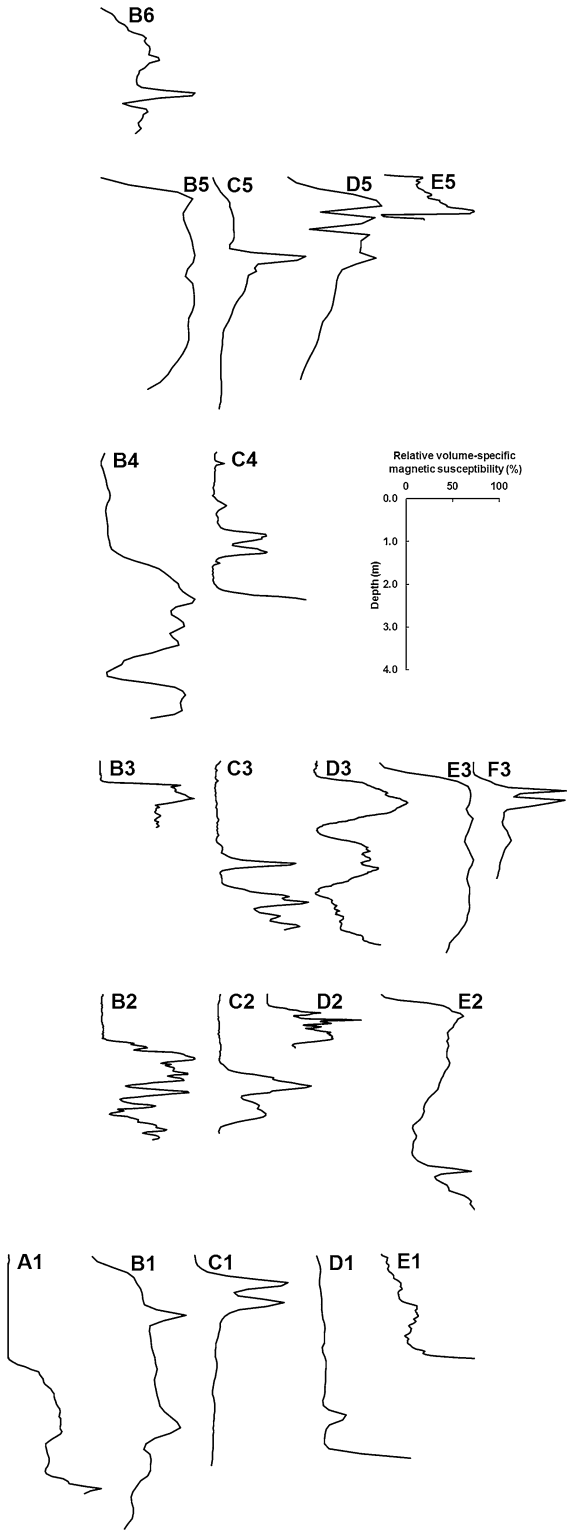

◀**Fig. 10** The magnetostratigraphy of Lake Lanotō and its surrounding swamps, southeast Upolu, Samoa. The logs represent measurements of volume-specific magnetic susceptibility made on cores taken from the basin. The locations of the cores are shown in Fig. 3. In order to ensure that the detail of each core's susceptibility signal is represented, the relative susceptibility of each core was calculated and expressed as a percentage

and the maximum value of susceptibility in each core (Fig. 14). This suggests that both peak susceptibility and unit thickness decrease progressively with distance from the edge of the accumulation zone. Unfortunately, this relationship can be no more than indicative as a number of the cores did not penetrate the entire thickness of the high-susceptibility unit: several of the data points in Fig. 14 therefore represent minimum values only. Notwithstanding this, Fig. 14 strongly suggests that the lower values of peak susceptibility found further into the basin are associated with a reduction in the thickness of the high-susceptibility unit.

Discussion

Processes of sediment accumulation in the volcanic crater

Peak magnetic susceptibility in the cores taken from the accumulation zone reaches values $> 300 \times 10^{-5}$ SI units, with the pattern of peak susceptibility indicative of the introduction of high-susceptibility material to the accumulation zone from the surrounding slopes (Fig. 13). Although the distribution of susceptibility across the crater floor might be interpreted as the product of bedrock reworked from the crater's flanks, only the soils, with a mean volume-specific magnetic susceptibility of 302×10^{-5} SI units ($s = 134 \times 10^{-5}$ SI units), could have supplied magnetically suitable material to the crater floor from the surrounding slopes.

One difficulty with this thesis is that some of the cores around the margins of the accumulation zone display peak susceptibilites $> 1000 \times 10^{-5}$ SI units (Fig. 13), above that of even the highest values of the soils (Table 1). It is likely, however, that the magnetic susceptibility of the soils, which represent samples of the plant-organic-rich, upper 0.15 m of the regolith on

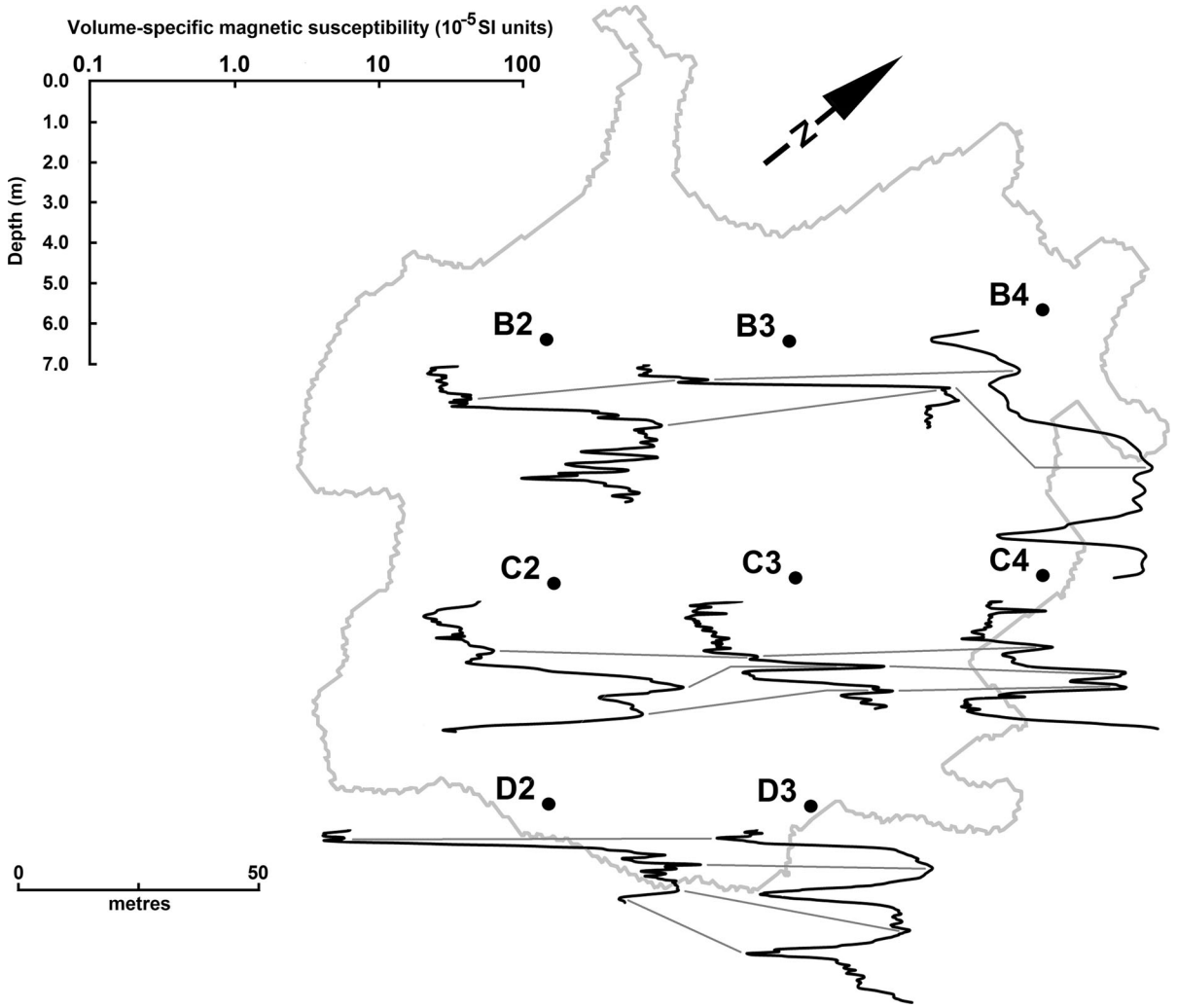

Fig. 11 The correlation of stratigraphic features in the sediments of Lake Lanotō, southeast Upolu, Samoa on the basis of measurements of volume-specific magnetic susceptibility made on the cores taken from the lake basin. Because of space constraints, only the most important stratigraphic tie lines are shown

the catchment slopes, has been diluted by the presence of diamagnetic plant matter. To assess this, we normalised the measured magnetic susceptibility values of the soils to take account of their plant-organic content (as estimated by loss on ignition). Few measurements have been made of the susceptibility of plant-organic sediments uncontaminated either by clastic matter or by pollutants. However, Longman et al. (2017) reported measurements of around -2×10^{-5} SI units from unpolluted peats possessing loss on ignition values of 86–94%. We employed this value to estimate the susceptibility of the mineral component of the soils on the interior slopes of the crater (Table 1). The values obtained are comparable with the maximum values recorded in the cores from the accumulation zone, supporting the proposition that the high-susceptibility deposits consist of soils and other regolith material moved down the catchment slopes and deposited on the margins of the accumulation zone.

Our chemical analyses shed additional light on the pattern of basin-floor sedimentation. The major element chemistry of the bedrock differs significantly from that of the sediments. However, the chemistry of the soils is closely comparable with that of the sediments in the lake (Fig. 9). This suggests that the

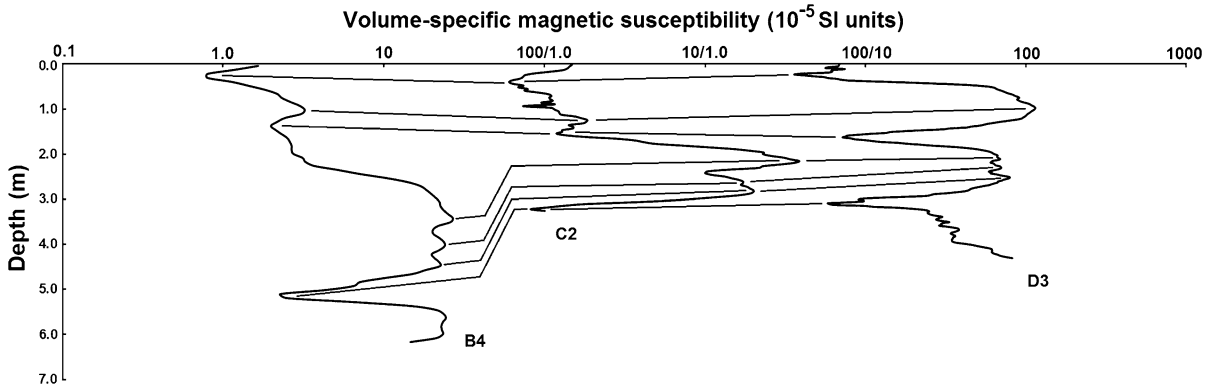

Fig. 12 The correlation of stratigraphic features in the sediments of cores B4, C2 and D3 from Lake Lanotō, southeast Upolu, Samoa on the basis of measurements of volume-specific magnetic susceptibility. The three cores are the deepest on each of the transects that cross the lake. They were selected to show the detail of the magnetostratigraphy of the lake sediments

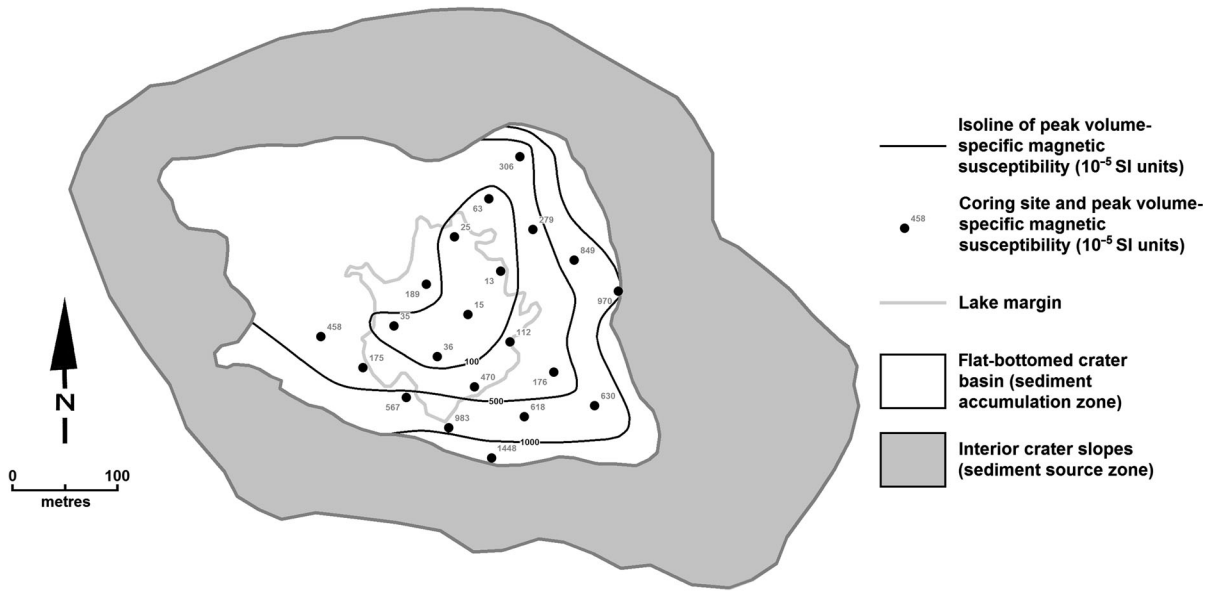

Fig. 13 The catchment of the interior basin of the volcanic cone of Mount Lanotō, southeast Upolu, Samoa, showing the pattern of peak values of volume-specific magnetic susceptibility recorded in each of the sediment cores taken from the basin

chemical signature of the slope material extends into the most distal part of the accumulation zone.

There is no evidence of gullying or channelisation of either the interior slopes of the basin or the deposits of the swamplands. The movement of the soil and regolith into the accumulation zone is therefore unlikely to have involved fluvial processes. Instead, it is likely that the material was moved by mass wasting, the result of the bulk movement of regolith material down the slopes under the direct influence of gravity.

The spatial pattern of peak magnetic susceptibility, the identification of the source of the high-susceptibility unit as soil and other regolith material reworked from the flanks of the basin, the decrease in thickness of the unit with distance into the basin and the absence of evidence of fluvial activity are suggestive of the operation of slope processes depositing material on the basin floor in the form of low-angle fans. The chemistry of the lake sediments suggests that deposits associated with these fans

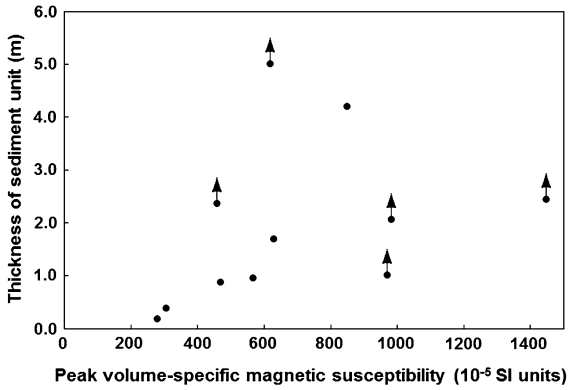

Fig. 14 The thickness of the high magnetic-susceptibility sediment unit in the cores taken from the interior basin of the volcanic cone of Mount Lanotō, southeast Upolu, Samoa and the maximum value of volume-specific magnetic susceptibility in each core. The high-susceptibility unit was defined as including all parts of the core possessing values of volume-specific magnetic susceptibility $\geq 190 \times 10^{-5}$ SI units. In five of the cores the base of the high-susceptibility unit was not reached. The values shown here are thus minima. They are depicted with an arrow to show the likely shift in the values of the thickness of the sediment unit

extended across the entire extent of the accumulation zone and into the central pit crater.

The decline in peak susceptibility values with distance into the accumulation zone is likely to be a consequence of the progressive deposition of the ferrimagnetic-rich input of regolith reworked from the interior slopes. With distance from the base of the slopes, the deposits of the accumulation zone would have become increasingly dominated by autochthonous plant-organic-rich material, with diamagnetic-rich background deposition diluting the high-susceptibility input.

We therefore envisage deposition taking place across the basin floor as a result of the mobilisation of soils and regolith materials from the steep inner slopes of the basin and its deposition in the form of low-angle fans in the accumulation zone. The fans would have become progressively thinner with distance into the swamplands. Peak susceptibility would also have declined, probably because of the preferential deposition of the ferrimagnetic-rich regolith input on the margins of the accumulation zone.

The high-susceptibility unit in the swamp cores displays up to three peaks (Fig. 10), suggesting that the injection of material into the swamplands occurred in several phases. Individual susceptibility peaks can be traced from the margins of the swamplands into the lake, the peaks becoming less pronounced with distance. This can be seen most clearly along transect C where peaks $> 500 \times 10^{-5}$ SI units in core C1 decline to $< 40 \times 10^{-5}$ SI units in C2 and $< 20 \times 10^{-5}$ SI units in C3 (Fig. 15). More broadly, the record from core D3 indicates that deposition in the lake, and perhaps across the swamplands as a whole, may have alternated between two states, one characterised by relatively high plant-organic content ($> 50\%$ loss on ignition) and relatively low mass-magnetic susceptibility, the other by a lower plant-organic content ($< 30\%$ loss on ignition) and relatively high mass-magnetic susceptibility (Fig. 16), with relatively abrupt jumps between the two states (particularly in the case of loss on ignition). The susceptibility peaks can be traced across all the cores in the lake basin. Each of these peaks appears to mark

Table 1 The volume-specific magnetic susceptibility, loss on ignition and mineral-matter-normalised magnetic susceptibility of the soils in the main crater of Mount Lanotō, southeast Upolu, Samoa

Soil sample	Low-frequency volume-specific magnetic susceptibility (10^{-5} SI units)	Loss on ignition (% by mass)	Mineral-matter-normalised low-frequency volume-specific magnetic susceptibility (10^{-5} SI units)
A	293	23.4	391
B	203	36.0	322
C	103	36.7	168
D	310	33.8	474
E	490	51.5	1014
F	268	30.5	392
I	448	32.7	672

The location of the soil sampling sites is shown in Fig. 3

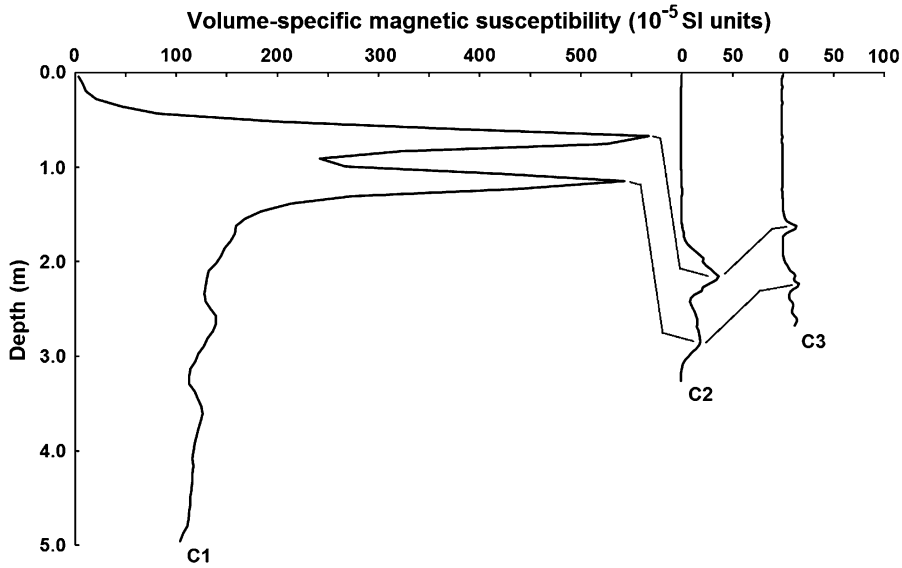

Fig. 15 The correlation of stratigraphic features in the sediments of cores C1, C2 and C3 from the flat-bottomed interior basin of the volcanic cone of Mount Lanotō, southeast Upolu, Samoa on the basis of measurements of volume-specific magnetic susceptibility

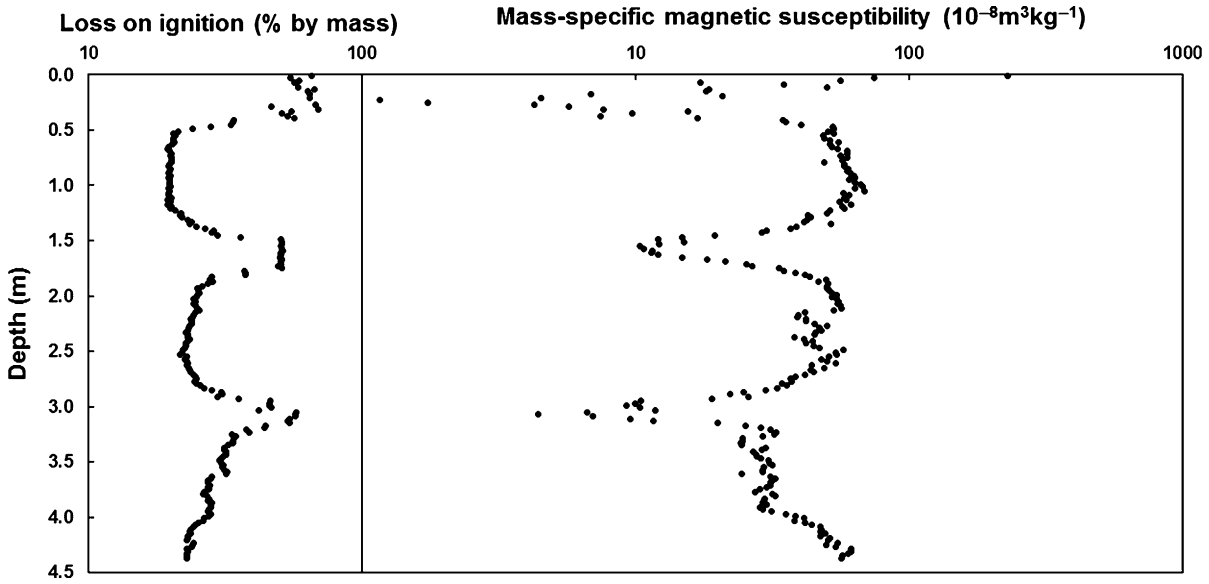

Fig. 16 The loss on ignition and mass-specific magnetic susceptibility of core D3 from Lake Lanotō, southeast Upolu, Samoa

an individual sedimentation event and is likely to represent the distal part of the low-angle fans inferred to have existed across the crater floor. The inter-peak units, on the other hand, may represent phases when mineral input to the system was reduced and when deposition was dominated by the accumulation of plant-organic material. This interpretation implies that, even in the central lake basin, the drivers of stratigraphic change are episodes of erosion on the steep slopes surrounding the accumulation zone.

The pattern of detrital sedimentation across the swamplands is likely to have been localised, with deposition in one sector not necessarily occurring concurrently with deposition elsewhere in the accumulation zone. This may explain the complexity of the swampland magnetostratigraphy (Fig. 10) and the

difficulty of establishing stratigraphic ties across the entire swamp area. Notwithstanding this, it appears that any deposition of material in the accumulation zone as a result of a localised mass-wasting event is also likely to have left a sedimentary signature in the central lake basin. The coherent stratigraphy of the central lake cores strongly suggests that they integrate the erosion record for the entire basin.

Despite the evidence for sedimentation across the base of the main crater, the sub-cylindrical pit of Lake Lanotō has remained open. This may be because the bulk of the sediment reworked from the crater slopes is deposited close to the margins of the accumulation zone, with little reaching the lake itself.

A model of post-eruptive sediment accumulation in Lake Lanotō

Although we have no direct evidence of its products, the earliest post-eruptive depositional event in the basin is likely to have been the result of the failure of the oversteepened internal slopes of the crater. Depending on the processes involved, the deposits may have taken the form of slumped blocks or fans of rock or debris. Given the scale of the failure surfaces, it is probable that the deposits would have covered the entire floor of the internal basin of the volcano.

At some stage thereafter, the floor of the basin appears to have collapsed to form a pit crater. The basal deposits in the pit crater are likely to be the product of the collapse of its walls and roof, although the upper 6 m of sediment in the pit were deposited in a lacustrine environment. Nevertheless, the basin is not likely to have experienced lacustrine conditions throughout its history, for Lake Lanotō is detached from the regional groundwater system: the late Quaternary volcanic rocks on which it is formed are highly permeable and the regional water table is deep and of low gradient (Kear and Wood 1959). The lake is therefore unlikely to have received regional groundwater recharge. Instead, the basin appears to have been partly sealed, either by its basal deposits or by more recent, plant-organic-rich muds, allowing filling by direct recharge by rainfall. The modern water balance at the site (daily rainfall minus daily potential evapotranspiration) is of the order of 2 m a^{-1}. Although we cannot speculate on how this value may have varied through the late Quaternary, this is easily adequate to fill the basin in decades or less, assuming negligible seepage loss.

During at least the later stages of sedimentation, the pit crater is likely to have experienced open-water conditions. Shallow water levels, in which swamp-like deposits were able to accumulate, may have existed concurrently across the rest of the accumulation zone. Deposition across the accumulation zone during this stage appears to have been dominated by autochthonous plant-organic-rich material, with minor fine-grained clastic input. This was intermittently interrupted by localised episodes of mass movement that introduced the regolith mantling the steep internal slopes of the crater into the swamp in the form of low-angle fans. Although the deposits of each episode were probably restricted to that part of the crater floor adjacent to the source of the eroded material, it is likely that the distal parts of each fan reached the lake. The lake sediment sequence therefore integrates the products of erosive events across the entire catchment.

Comparison with models of caldera and maar sedimentation

In addition to their volcanic context, volcanic crater lakes have many characteristics in common with volcanic calderas and maars. These include their small catchments, their isolation from the surrounding environment by the topographic barrier of the crater rim, and their steep, failure-prone internal slopes. Nevertheless, there are notable differences. Volcanic calderas (particularly that at the type site of Crater Lake) are exceptionally steep-sided and possess considerable relief. Their water bodies are usually considerably larger and deeper than those of volcanic craters. They tend to experience complex volcanic (and associated tectonic) histories that may precede and overlap with the lake sedimentation phase (Chesner 2012; Goto et al. 2015).

By contrast, maar lakes offer a closer comparison with true crater lakes. The lakes are similar in size, straightforward in form and have simple volcanic histories, although maars are usually of lower relief and have lower marginal rims than volcanic craters. Their permeable roots, composed of rock fragments, ash and other ejecta, and the excavation of their craters below the pre-eruptive surface give them a direct hydraulic connection with the groundwater system. Such links seldom exist in volcanic crater lakes, which

are often perched above the water table. One consequence of this is that maars experience lacustrine conditions early in their development and may flood rapidly immediately after eruption. Lacustrine depositional environments are therefore initiated more quickly in maars than in calderas (and, possibly, volcanic craters) and they tend not to experience a protracted phase of pre-lacustrine subaerial deposition.

The broad picture of sedimentation in all three types of volcanic lake is similar. The earliest, post-eruptive, deposits often consist of tens of metres of coarse, lithic material resulting from the collapse of oversteepened crater walls. This is succeeded by fine-grained lake sediments, particularly in the deeper and more distal parts of the basin. Around the margins of the accumulation zone, the lake sediments are interfingered by mass-movement deposits, including turbidites and low-angle debris fans. These wedge into the lake sediments and have their source on the steeper and more unstable margins of the basin. All three types of lake are likely to be located in volcanically active terrains and will thus experience intermittent ash falls and the incorporation of tephra in the lacustrine sequence. With the exception of such aeolian contributions, however, the clastic deposits in volcanic crater lakes are derived solely from the by-products of the volcanic eruption. Maars and volcanic calderas, by contrast, are developed within the country rock and their clastic sediments may contain large amounts of non-volcanic material eroded from the crater walls (Büchel and Pirrung 1993; Otake 2007).

The pattern of deposition in volcanic calderas is complicated by the existence of localised basins that focus sedimentation and experience marginal sedimentary processes, and by continuing volcanic and tectonic activity that alters basin geomorphology and adds new sediment sources. Volcanic calderas also appear to experience a long and complicated episode of subaerial deposition prior to the initiation of lacustrine conditions.

Maars, by contrast, generally have simple morphologies so the pattern and nature of their sedimentation tends to be uncomplicated. The steep walls and small size of maar lakes makes them susceptible to permanent or semi-permanent stratification. Under such conditions, the bottom waters of the lakes are perennially anoxic, with the absence of burrowing benthic organisms favouring the deposition of fine-grained, annually laminated lake sediments. Both maar and caldera lakes are typically rather deep and steep sided and often biologically unproductive. By contrast, it is not unusual for volcanic crater lakes to be relatively shallow and biologically productive, potentially yielding autochthonous, plant-organic-rich sediments of the sort that dominate the basin of Lake Lanotō.

Conclusions

The young volcanic landscapes of the two largest islands of the Samoan chain possess almost 400 volcanic cones. Many of these form enclosed, internally drained basins capable of retaining long, detailed and uninterrupted sedimentary sequences. Because of the sparsity, fragmentary nature and low temporal resolution of records of environmental change from the tropical Pacific, these deposits have the potential to fill an important gap in our knowledge of global climatic and environmental change.

To interpret these records we need to understand the depositional processes that operate in these basins. Unfortunately, although the post-eruptive sedimentology of volcanic calderas and maars is relatively well-established, that of crater lakes such as those found on Savai'i and Upolu remains poorly understood.

A relatively simple volcanic edifice, Mount Lanotō in southeast Upolu, was selected for detailed investigation. The sediments of the crater basin are composed largely of plant-organic-rich muds that display little visible evidence of stratigraphic variation. Mineral magnetic and chemical methods were therefore employed to identify spatial and vertical changes in sediment character. This information was used to document the types and distribution of sedimentary facies represented in the post-eruptive crater fill and, by inference, the processes of sedimentation that had operated in the crater.

The earliest post-eruptive deposits are likely to have been the product of the failure of the crater's oversteepened internal slopes. The floor of the basin subsequently appears to have collapsed to form a pit crater. Although the basal deposits in the pit crater are likely to be the product of the collapse of its walls and roof, the bulk of the material in the feature was laid down under open-water lacustrine conditions. At the same time, shallow-water conditions may have existed

across the rest of the accumulation zone. Sedimentation during this stage appears to have been dominated by autochthonous plant-organic-rich deposits, with minor fine-grained clastic input. These conditions were intermittently interrupted by localised episodes of mass movement that reworked the regolith mantling the steep internal slopes of the crater into the swamp in the form of low-angle fans. Although the deposits of each mass-movement episode were probably restricted to that part of the crater floor adjacent to the erosion source, it is likely that the distal parts of each fan reached the lake. The lake deposits may therefore integrate the products of erosive events across the entire catchment.

At the broad scale, the sedimentology of Lake Lanotō displays similarities with that of caldera and maar lakes: coarse, mass-wasting deposits resulting from the collapse of the oversteepened crater walls are succeeded by fine-grained lacustrine sediments. Around the margins of the accumulation zone, the lake sediments are interfingered by the deposits of low-angle fans. These wedge into the lake sediments and have their source on the steeper and more unstable margins of the basin. Nevertheless, there are important differences. Crater lakes and maars are morphologically simple and do not possess the pattern of multiple basins found in volcanic calderas. They therefore display a simple pattern of sedimentation. Nor do maars and craters tend to experience contemporaneous volcanic activity, which adds new sediment sources to caldera lake systems, changes the form of the caldera's depositional basin and intercalates volcanic material with the caldera sediments.

The timing of flooding and the onset of lacustrine conditions are likely to have differed between the three lake types. In particular, volcanic calderas appear to experience a long and complicated episode of subaerial deposition prior to the initiation of lacustrine conditions. By contrast with calderas and maars, the clastic deposits in volcanic crater lakes are derived almost solely from the by-products of the volcanic eruption, whilst the rather deep and steep-sided form of maar and caldera lakes tends to inhibit biological productivity so that it is rare to find autochthonous, plant-organic-rich sediments of the sort that dominate the basin of Lake Lanotō.

Our data from Lake Lanotō add to the limited amount of information on post-eruptive sedimentation in volcanic crater lakes and provide valuable insight into the interpretation of the environmental record preserved in this and similar sites. There are important differences between the types and distribution of sedimentary facies identified at Lake Lanotō and those represented in models of deposition in maars and volcanic calderas. Nevertheless, we are far from establishing a widely applicable model of sedimentation in volcanic craters, and further work in a range of environments will be required before this is possible. Notwithstanding this, our results may be sufficiently general to help in the interpretation of other ancient and modern lacustrine environments.

Acknowledgements AF acknowledges the support of a Graduate Assistant Scholarship from The University of the South Pacific. AF and SJG acknowledge funding from the Faculty of Science, Technology and Environment of The University of the South Pacific. We thank Seulgee Samuelu of the Alafua Campus of The University of the South Pacific for her help in Samoa, and the staff of the School of Agriculture and Food Technology of the Alafua Campus of The University of the South Pacific for granting us permission to use their laboratory facilities. Associate Professor Karoly Németh carefully read an earlier draft of the manuscript and Dr. Art Whistler generously shared with us the results of his botanical survey of the Lake Lanotō basin. We are especially grateful to the Palea Vea family from Lepā in Upolu for their hospitality and for all their help with this project.

References

Büchel G, Pirrung M (1993) Tertiary maars of the Hocheifel Volcanic Field, Germany. In: Negendank JFW, Zolitschka B (eds) Paleolimnology of European maar lakes. Springer, Berlin, pp 447–465

Burgess SM (ca 1987) The climate and weather of Western Samoa. New Zealand Meteorological Service Miscellaneous Publication 188(8)

Chesner CA (2012) The Toba Caldera Complex. Quat Int 258:5–18

Christenson BW, Németh K, Rouwet D, Tassi F, Vandemeulebrouck J, Varekamp JC (2015) Volcanic lakes. In: Rouwet D, Christenson BW, Tassi F, Vandemeulebrouck J (eds) Volcanic lakes. Springer, Berlin, pp 1–20

Cohen AS (2003) Paleolimnology: the history and evolution of lake systems. Oxford University Press, New York

Dana JD (ca 1849) United States exploring expedition. During the years 1838, 1839, 1840, 1841, 1842. Under the command of Charles Wilkes, U.S.N. Geology. G. P. Putnam, New York

de Wall H, Worm H-U (2000–2001) A cautionary note on interpreting frequency-dependence of susceptibility solely in terms of superparamagnetism or two ways to be wrong. Inst Rock Magn Q 10(4):1, 6–7

Dearing JA (1999) Environmental magnetic susceptibility using the Bartington MS2 system, 2nd edn. Chi Publishing, Kenilworth

Department of Lands and Survey, Western Samoa (1978) Lepā. Western Samoa Topographical Map 1:20,000 Upolu Sheet 27, 2nd edn. Department of Lands and Survey, Government of Samoa, Apia

EarthRef (2006) Samoan hotspot trail region-130S-1763W–Pacific Ocean predicted bathymetric map. http://erda.sdsc.edu/maps/SAM/JPG/REGION-130S-1763W.std.1380m.ss.map.jpg

Gale SJ, Hoare PG (2011) Quaternary sediments: petrographic methods for the study of unlithified rocks, 2nd edn. Blackburn Press, New Jersey

Gale RJB, Gale SJ, Winchester HPM (2006) Inorganic pollution of the sediments of the River Torrens, South Australia. Environ Geol (Berl) 50:62–75

Goto Y, Matsuzuka S, Kameyama S, Danhara T (2015) Geology and evolution of the Nakajima Islands (Toya Caldera, Hokkaido, Japan) inferred from aerial laser mapping and geological field surveys. Bull Volcanol Soc Jpn 60:17–33

Guo ZF, Liu JQ, Fan QC, He HY, Sui SZ, Chu GQ, Liu Q, Negendank JFW (2005) Source of volcanic ash in the sediments of Sihailongwan maar lake, NE China, and its significance. Acta Petrol Sin 21:251–255

Hart SR, Coetzee M, Workman RK, Blusztajn J, Johnson KTM, Sinton JM, Steinberger B, Hawkins JW (2004) Genesis of the Western Samoa seamount province: age, geochemical fingerprint and tectonics. Earth Planet Sci Lett 227:37–56

Heiken G, Krier D, McCormick T, Snow MG (2000) Intracaldera volcanism and sedimentation—Creede caldera, Colorado. In: Bethke PM, Hay RL (eds) Ancient Lake Creede: its volcano-tectonic setting, history of sedimentation, and relation to mineralization in the Creede mining district. Geological Society of America Special Paper 346, pp 127–157

Holmgren SU, Ljung K, Björck S (2012) Late Holocene environmental history on Tristan da Cunha, South Atlantic, based on diatom floristic changes and geochemistry in sediments of a volcanic crater lake. J Paleolimnol 47:221–232

Jiang BY, Fürsich FT, Hethke M (2012) Depositional evolution of the Early Cretaceous Sihetun Lake and implications for regional climatic and volcanic history in western Liaoning, NE China. Sediment Geol 257–260:31–44

Kear D, Wood BL (1959). The geology and hydrology of Western Samoa. N Z Geol Surv Bull NS 63

Köppen WP (1936) Das geographische system der klimate. In: Köppen WP, Geiger R (eds) Handbuch der klimatologie, band 1, teil C. Gebrüder Borntraeger, Berlin

Larsen D, Crossey LJ (1996) Depositional environments and paleolimnology of an ancient caldera lake: Oligocene Creede Formation, Colorado. Geol Soc Am Bull 108:526–544

Longman J, Veres D, Ersek V, Salzmann U, Hubay K, Bormann M, Wennrich V, Schäbitz F (2017) Periodic input of dust over the Eastern Carpathians during the Holocene linked with Saharan desertification and human impact. Climate of the Past Discussions. https://doi.org/10.5194/cp-2017-6

Lorenz V (1973) On the formation of maars. Bull Volcanol (Rome) 37:183–204

Lorenz V (2007) Syn- and posteruptive hazards of maar–diatreme volcanoes. J Volcanol Geotherm Res 159:285–312

McDougall I (2010) Age of volcanism and its migration in the Samoa Islands. Geol Mag 147:705–717

Mena M, Ré GH, Haller MJ, Singer SE, Vilas JF (2006) Paleomagnetism of the late Cenozoic basalts from northern Patagonia. Earth Planets Space 58:1273–1281

Murphy BS, Gaines RR, Lackey JS (2016) Co-evolution of volcanic and lacustrine systems in Pleistocene Long Valley Caldera, California, U.S.A. J Sediment Res 86:1129–1146

Natland JH, Turner DL (1985) Age progression and petrological development of Samoan shield volcanoes: evidence from K-Ar ages, lava compositions, and mineral studies. In: Brocher TM (ed) Investigations of the northern Melanesian borderland. Circum-Pacific Council for Energy and Mineral Resources Earth Science Series Volume 3. Circum-Pacific Council for Energy and Mineral Resources, Houston, pp 139–171

Nelson CH, Bacon CR, Robinson SW, Adam DP, Bradbury JP, Barber JH, Schwartz D, Vagenas G (1994) The volcanic, sedimentologic, and paleolimnologic history of the Crater Lake caldera floor, Oregon: evidence for small caldera evolution. Geol Soc Am Bull 106:684–704

Németh K, Cronin SJ (2008) Volcanic craters, pit craters and high-level magma-feeding systems of a mafic island-arc volcano: Ambrym, Vanuatu, South Pacific. In: Thomson K, Petford N (eds) Structure and emplacement of high-level magmatic systems. Geological Society, London, Special Publications 302, pp 87–102

O'Reilly CM, Sharma S, Gray DK, Hampton SE, Read JS, Rowley RJ, Schneider P, Lenters JD, McIntyre PB, Kraemer BM, Weyhenmeyer GA, Straile D, Dong B, Adrian R, Allan MG, Anneville O, Arvola L, Austin J, Bailey JL, Baron JS, Brookes JD, de Eyto E, Dokulil MT, Hamilton DP, Havens K, Hetherington AL, Higgins SN, Hook S, Izmest'eva LR, Joehnk KD, Kangur K, Kasprzak P, Kumagai M, Kuusisto E, Leshkevich G, Livingstone DM, MacIntyre S, May L, Melack JM, Mueller-Navarra DC, Naumenko M, Noges P, Noges T, North RP, Plisnier P-D, Rigosi A, Rimmer A, Rogora M, Rudstam LG, Rusak JA, Salmaso N, Samal NR, Schindler DE, Schladow SG, Schmid M, Schmidt SR, Silow E, Soylu ME, Teubner K, Verburg P, Voutilainen A, Watkinson A, Williamson CE, Zhang G (2015) Rapid and highly variable warming of lake surface waters around the globe. Geophys Res Lett 42:10,773–10,781

Öberg H, Andersen TJ, Westerberg L-O, Risberg J, Holmgren K (2012) A diatom record of recent environmental change in Lake Duluti, northern Tanzania. J Paleolimnol 48:401–416

Okubo CH, Martel SJ (1998) Pit crater formation on Kilauea volcano, Hawaii. J Volcanol Geotherm Res 86:1–18

Ollier CD (1967) Maars their characteristics, varieties and definition. Bull Volcanol (Heidelberg) 31:45–73

Otake M (2007) Sedimentary facies, processes and environments of the Akakura caldera lake, the South Kurikoma geothermal area, northeast Japan. J Geol Soc Jpn 113:549–564

PAGES2k Consortium (2017) A global multiproxy database for temperature reconstructions of the Common Era. Sci Data 4:170088

Parkes A (1994) Holocene environments and vegetational change on four Polynesian islands. Unpublished Ph.D. thesis, University of Hull, Hull, 204 + 233 pp

Pirrung M, Fischer C, Büchel G, Gaupp R, Lutz H, Neuffer F-O (2003) Lithofacies succession of maar crater deposits in the Eifel area (Germany). Terra Nova 15:125–132

Pollard J-PJ, Sherwood GJ, Böhnel H (1998) Preliminary results from rock magnetic analyses of Quaternary and Tertiary basalts from the Gulf Coast of Mexico. Geol Carpathica 49:5–14

Ross P-S, Delpit S, Haller MJ, Németh K, Corbella H (2011) Influence of the substrate on maar–diatreme volcanoes—an example of a mixed setting from the Pali Aike volcanic field, Argentina. J Volcanol Geotherm Res 201:253–271

Solofa D, Aung T (2004) Samoa's 102 year meteorological record and a preliminary study on agricultural product and ENSO variability. South Pac J Nat Sci 22:46–50

Stearns HT (1944) Geology of the Samoan islands. Bull Geol Soc Am 55:1279–1331

Timms BV (1992) Lake geomorphology. Gleneagles, Adelaide

White JDL (1989) Basic elements of maar-crater deposits in the Hopi Buttes volcanic field, northeastern Arizona, USA. J Geol (Chicago) 97:117–125

White JDL (1992) Pliocene subaqueous fans and Gilbert-type deltas in maar crater lakes, Hopi Buttes, Navajo Nation (Arizona), USA. Sedimentology 39:931–946

White JDL, Ross P-S (2011) Maar-diatreme volcanoes: a review. J Volcanol Geotherm Res 201:1–29

Workman RK, Hart SR, Jackson MG, Regelous M, Farley KA, Blusztajn J, Kurz M, Staudigel H (2004) Recycled metasomatized lithosphere as the origin of the Enriched Mantle II (EM2) end-member: evidence from the Samoan Volcanic Chain. Geochem Geophys Geosyst 5(4):Q04008. https://doi.org/10.1029/2003GC000623

Wyrick D, Ferrill DA, Morris AP, Colton SL, Sims DW (2004) Distribution, morphology, and origins of Martian pit crater chains. J Geophys Res: Planets 109(E6):E06005. https://doi.org/10.1029/2004JE002240